УДК 519.6

Turbulence Model for Supersonic Turbulent Flows with Variable Composition*

A. M. Molchanov, L. V. Bykov

Moscow Aviation Institute (State University of Aerospace Technologies), Moscow;
e-mail: alexmol_2000@mail.ru

A new turbulence model based on the assumption that the velocity fluctuations directed normal to streamwise play a key role in turbulent mixing process is presented. Analyzing Reynolds stress equations and introducing the weak-equilibrium assumption for the members comprised in these equations resulted in simple equations for Reynolds stress. The model involves turbulent kinetic energy and turbulent dissipation rate equations (k-e) including compressibility corrections. A turbulence model allowing the calculation of the variable turbulent Prandtl (Prt) and Schmidt (Sct) numbers as part of the solution is presented. For the validation of the code the described numerical procedures are applied to a series of jet flow problems. These include over- and under-expanded cold and hot free jets, supersonic combustion of hydrogen in a vitiated air, afterburning of hot-gas generator plumes. Comparison of the simulation with available experimental data showed a good agreement for the above problems.

Keywords: turbulence, supersonic, compressibility corrections, variable turbulent Prandtl and Schmidt numbers, turbulent Mach number, normal velocity fluctuations.

Introduction

The turbulence models developed for incompressible flows fail to describe high-speed compressible flows very well. As known, compressibility in high-speed flows has a stabilizing influence on turbulence so that the intensity of turbulent mixing reduces as Mach number increases.

This effect plays an important role in present-day problems of rocket and airspace engineering. For example, in a supersonic combustion ramjet reduced turbulence levels can be highly detrimental as they reduce the rate at which fuel and oxidizer mix. Compressibility changes the nature of laminar-turbulent boundary-layer transition over hypersonic vehicles during re-entry.

The turbulent Prandtl and Schmidt numbers have a significant influence on heat flux and turbulent diffusion at supersonic reacting flows. Experimental data show that turbulent Prandtl and Schmidt numbers may vary within quite a big range.

To consider this phenomenon the author suggests a turbulence model that considers the impact of compressibility effects on turbulence and allows for the calculation of the variable turbulent Prandtl and Schmidt numbers as part of the solution.

* The Financial Supports from Russian Foundation for Basic Research (Grant RFBR No 11-08-00828-a).

Governing equations

The set of equations for high Reynolds two-dimension turbulent reacting flow is described in the Reference [1].

It includes continuity equation, two momentum equations, energy equation, species continuity equations and the equations of the turbulence model.

Turbulence Model

The standard turbulent models developed for incompressible flows over predict turbulence levels, and hence mixing rates, because it does not account for the effects of compressibility on turbulence dissipation.

It is supposed that pressure fluctuation appearing in the mixing layer when subsonic and supersonic gas volumes interact causes supplementary dissipation.

In terms of mathematical modeling this effect accounts for the fact that apart from solenoidal dissipation $\overline{\rho}\varepsilon$, in the transport equation for K additional members appear [2]:

1) compressible dissipation

$$\overline{\rho}\varepsilon_C = \frac{4}{3}\overline{\mu}\overline{d''^2}, \qquad (1)$$

2) correlation between the pressure and divergence fluctuations

$$\kappa = \overline{p'd''}, \tag{2}$$

where d'' — velocity divergence fluctuation.

Sarkar et al. [2], and Zeman [3] showed that moderate compressibility does not affect the solenoidal part of dissipation and the same transport equation as in case of incompressible flow can be applied to it.

Sarkar et al. [2] formula is most often used for modeling additional members:

$$\bar{\rho}\varepsilon_C - \kappa = \alpha_1 M_T^2 \bar{\rho}\varepsilon, \tag{3}$$

where M_T — Mach turbulent number,

$$M_T = \frac{\sqrt{2K}}{a}, \tag{4}$$

a — local sound speed, $\alpha_1 = 1$ — numerical constant.

The earlier paper of Glebov and Molchanov [4] used the formula:

$$\bar{\rho}\varepsilon_C - \kappa = C_M \bar{\rho} M_T \varepsilon, \tag{5}$$

where $C_M = 0.29$ — numerical constant.

Formulae (3) и (5) have the same form:

$$\bar{\rho}\varepsilon_C - \kappa = \varphi(M_T)\bar{\rho}\varepsilon, \tag{6}$$

where $\varphi(M_T)$ — compressibility function.

There are some more formulae for this compressibility function (for example, Refs. [5, 6]).

Thus, the transport equations for K and ε for high Reynolds numbers are as follows

$$\frac{\partial}{\partial t}(\bar{\rho}K) + \frac{\partial}{\partial x_j}(\bar{\rho}\tilde{u}_j K) = \frac{\partial}{\partial x_j}\left[\frac{\mu_T}{\sigma_K}\frac{\partial K}{\partial x_j}\right] + P_K - \left[1+\varphi(M_T)\right]\bar{\rho}\varepsilon, \tag{7}$$

$$\frac{\partial}{\partial t}(\bar{\rho}\varepsilon) + \frac{\partial}{\partial x_j}(\bar{\rho}\tilde{u}_j \varepsilon) = \frac{\partial}{\partial x_j}\left[\left(\frac{\mu_T}{\sigma_\varepsilon} + \mu\right)\frac{\partial \varepsilon}{\partial x_j}\right] + \frac{\varepsilon}{K}\left(C_{\varepsilon 1} P_K - C_{\varepsilon 2}\bar{\rho}\varepsilon\right), \tag{8}$$

which use standard constant pool:

$$\sigma_K = 1;\ \sigma_\varepsilon = 1.3;\ C_{\varepsilon 1} = 1.44;\ C_{\varepsilon 2} = 1.92. \tag{9}$$

In these equations P_K is the production term.

This paper uses the modification of K-ε turbulence model based on the analysis of transport equations for Reynolds stress.

Assuming that diffusion and convection are balanced in these equations, the following formula for turbulent viscosity can be obtained

$$\mu_T = \frac{(1-C_2)}{C_1}\frac{\widetilde{V_n''^2}}{K}\cdot\bar{\rho}\frac{K^2}{\varepsilon} = C_\mu \bar{\rho}\frac{K^2}{\varepsilon}, \tag{10}$$

where

$$C_\mu = \frac{(1-C_2)}{C_1}\frac{\widetilde{V_n''^2}}{K} = \frac{2}{3}\frac{(1-C_2)}{C_1}\left\{1 - \frac{(1-C_2)}{C_1}\left[1+\varphi(M_T)\right]\right\}, \tag{11}$$

V_n'' — velocity fluctuation normal to the streamlines, for which it is true:

$$\frac{\widetilde{V_n''^2}}{K} = \frac{2}{3}\left\{1 - \frac{(1-C_2)}{C_1}\left[1+\varphi(M_T)\right]\right\}. \tag{12}$$

The following numerical constants are used:

$$C_1 = 1.8;\ C_2 = 0.6. \tag{13}$$

Therefore, with the increase of flow velocity and corresponding increase of M_T the anisotropy of turbulence also increases (the ratio $\widetilde{V_n''^2}/K$ reduces).

Thus, unlike standard K-ε turbulence model, the presented model firstly includes supplementary dissipation dependable on the turbulent Mach number M_T, and secondly the coefficient C_μ in formula (10) of turbulent viscosity is no longer constant but dependable on M_T as well.

The following constant was used in formula (5) for this model:

$$C_M = 0.4. \tag{14}$$

Enthalpy, internal energy and species mass fractions are scalar values, so their turbulent fluxes are called *scalar fluxes*. Let's denote all scalar values by f.

As it was mentioned above scalar turbulent fluxes are most often closed by a classical Boussinesq-like formulation:

$$\widetilde{\bar{\rho}u_j'' f''} = -\frac{\mu_T}{\sigma_f}\frac{\partial \tilde{f}}{\partial x_j}, \tag{15}$$

where σ_f — a numerical coefficient.

For enthalpy: $\sigma_f = Pr_T$ — turbulent Prandtl number; for species mass fractions: $\sigma_f = Sc_T$ — turbulent Schmidt number. Usually it is assumed that: $Pr_T = Sc_T = 0.7$ for free shear layers and $Pr_T = Sc_T = 0.9$ for near-wall flows.

The turbulent Prandtl and Schmidt numbers have a significant influence on heat flux and turbulent diffusion in supersonic reacting flows. The typical assumption that they are constant and equal to each other is often inaccurate.

Numerous experimental data [7] showed that turbulent Prandtl and Schmidt numbers may vary within quite a big range: from 0.1 to 2.

Analyzing the transport equation for scalar value f turbulent flux and assuming that diffusion and convection are balanced in this equation, we can obtain the following formula for turbulent flux of scalar value in normal direction:

$$\widetilde{V_n'' f''} = -\frac{\widetilde{V_n''^2}}{K}\frac{\tau_f}{C_{1\varphi}} K \frac{\partial \tilde{f}}{\partial n}, \qquad (16)$$

where τ_f — time scale of turbulence. Usually the ratio K/ε is used for this time scale, which actually characterizes only velocity fluctuations. It would be more accurate to consider the time scale of scalar value fluctuations — ratio $\widetilde{f''^2}/\varepsilon_f$. Here ε_f — the dissipation rate of scalar value $\widetilde{f''^2}$.

This paper proposes using geometric average between these two time scales:

$$\tau_f = \sqrt{\frac{K}{\varepsilon}\frac{\widetilde{f''^2}}{\varepsilon_f}}. \qquad (17)$$

In formula (16) constant $C_{1\varphi} = 3.0$ [7].

The transport equations for $\widetilde{f''^2}$ and ε_f are as follows [8]:

$$\frac{\partial}{\partial t}\left(\bar{\rho}\widetilde{f''^2}\right) + \frac{\partial}{\partial x_j}\left(\bar{\rho}\tilde{u}_j \widetilde{f''^2}\right) =$$
$$= \frac{\partial}{\partial x_j}\left[\frac{\mu_T}{\sigma_{K,f}}\frac{\partial \widetilde{f''^2}}{\partial x_j}\right] + 2\frac{\mu_T}{\sigma_f}\left(\frac{\partial \tilde{f}}{\partial x_j}\right)^2 - 2\bar{\rho}\varepsilon_f, \qquad (18)$$

$$\frac{\partial}{\partial t}(\bar{\rho}\varepsilon_f) + \frac{\partial}{\partial x_j}(\bar{\rho}\tilde{u}_j\varepsilon_f) = \frac{\partial}{\partial x_j}\left[\frac{\mu_T}{\sigma_{\varepsilon,f}}\frac{\partial \varepsilon_f}{\partial x_j}\right] +$$
$$+\frac{\mu_T}{\sigma_f}\left(C_{d1}\frac{\varepsilon_f}{\widetilde{f''^2}} + C_{d2}\frac{\varepsilon}{K}\right)\left(\frac{\partial \tilde{f}}{\partial x_j}\right)^2 + \qquad (19)$$
$$+C_{d3}\frac{\varepsilon_f}{K}P_K - \bar{\rho}\varepsilon_f\left(C_{d4}\frac{\varepsilon_f}{\widetilde{f''^2}} + C_{d5}\frac{\varepsilon}{K}\right),$$

where constants are equal to [8]:

$$\begin{aligned} &\text{Cd1} = 2.0;\ \text{Cd2} = 0.0;\ \text{Cd3} = 0.72;\\ &\text{Cd4} = 2.2;\ \text{Cd5} = 0.8;\ \text{se, f} = 1;\ \text{sK, f} = 1. \end{aligned} \qquad (20)$$

Equation (19) is used as proposed in Ref. [8] but slightly altered because compressibility effect in this paper is considered in a different way.

When modeling turbulent diffusion fluxes, the species mass fractions Y_m are used as scalar value f:

$$f = Y_m. \qquad (21)$$

It is more convenient not to use equations (18), (19) for each species mass fraction separately but to solve equations governing the sum of the mass fraction variances and its dissipation rates:

$$\frac{\partial}{\partial t}(\bar{\rho}\varphi) + \frac{\partial}{\partial x_j}(\bar{\rho}\tilde{u}_j\varphi) =$$
$$= \frac{\partial}{\partial x_j}\left(\frac{\mu_T}{\sigma_{K,f}}\frac{\partial \varphi}{\partial x_j}\right) + 2P_\varphi - 2\bar{\rho}\varepsilon_\varphi, \qquad (22)$$

$$\frac{\partial}{\partial t}(\bar{\rho}\varepsilon_\varphi) + \frac{\partial}{\partial x_j}(\bar{\rho}\tilde{u}_j\varepsilon_\varphi) = \frac{\partial}{\partial x_j}\left[\frac{\mu_T}{\sigma_{\varepsilon,f}}\frac{\partial \varepsilon_\varphi}{\partial x_j}\right] +$$
$$+\left(C_{d1}\frac{\varepsilon_\varphi}{\widetilde{f''^2}} + C_{d2}\frac{\varepsilon}{K}\right)P_\varphi + C_{d3}\frac{\varepsilon_\varphi}{K}P_K - \qquad (23)$$
$$-\bar{\rho}\varepsilon_\varphi\left(C_{d4}\frac{\varepsilon_\varphi}{\varphi} + C_{d5}\frac{\varepsilon}{K}\right),$$

where

$$P_\varphi = \frac{\mu_T}{\mathrm{Sc}_T}\sum_{I=1}^{N_C}\frac{\partial \widetilde{Y_I}}{\partial x_j}\frac{\partial \widetilde{Y_I}}{\partial x_j},\quad \varphi = \sum_{I=1}^{N_C}\widetilde{Y_I''^2},\quad \varepsilon_\varphi = \sum_{I=1}^{N_C}\varepsilon_{C,I}. \qquad (24)$$

When modeling turbulent fluxes of enthalpy, only its thermodynamic part h_T is used as scalar value f.

The species enthalpy h_k consists of two quite different parts

$$h_I = h_{0,I} + \int_{T_0}^{T} C_{P,I}\,dT = h_{0,I} + h_{T,I}. \qquad (25)$$

The first part is species enthalpy of formation at a standard temperature T_0 and is essential for flows with chemical reactions. The second part for each species only depends on temperature; it is called species thermodynamic enthalpy.

The thermodynamic enthalpy of gas mixture is estimated as

$$h_T = \sum_{I=1}^{N_C} h_{T,I} Y_I. \qquad (26)$$

Such approach allows for distinguishing the effect of temperature fields on turbulence.

Thus, equations (18), (19) are used for the enthalpy variance $\widetilde{h_T''^2}$ and its dissipation rate ε_h.

From equations (10), (15), (16) and (17) one can derive the formula for σ_f:

$$\sigma_f = \frac{(1-C_2)C_{1\varphi}}{C_1}\sqrt{\frac{K}{\varepsilon}\frac{\varepsilon_f}{\widetilde{f''^2}}}. \qquad (27)$$

Particularly for turbulent Prandtl and Schmidt numbers we have:

$$\mathrm{Pr}_T = \frac{(1-C_2)C_{1\varphi}}{C_1}\sqrt{\frac{K}{\varepsilon}\frac{\varepsilon_h}{\widetilde{h_T''^2}}}, \quad (28)$$

$$\mathrm{Sc}_T = \frac{(1-C_2)C_{1\varphi}}{C_1}\sqrt{\frac{K}{\varepsilon}\frac{\varepsilon_\varphi}{\varphi}}. \quad (29)$$

As mentioned, the constants in the model are as follows:

$$\begin{aligned} &\sigma_K = 1; \quad \sigma_\varepsilon = 1.3; \quad C_{\varepsilon 1} = 1.44; \quad C_{\varepsilon 2} = 1.92; \\ &C_1 = 1.8; \quad C_2 = 0.6; \quad C_M = 0.4; \quad C_{1\varphi} = 3.0; \\ &C_{d1} = 2.0; \quad C_{d2} = 0.0; \quad C_{d3} = 0.72; \quad C_{d4} = 2.2; \\ &C_{d5} = 0.8; \quad \sigma_{\varepsilon,f} = 1; \quad \sigma_{K,f} = 1. \end{aligned} \quad (30)$$

Computational Results

For the validation of proposed turbulence model and numerical scheme six tests were performed.

The selection of each test case was based on two principles:

1) each test had to introduce an additional unique feature to be investigated;

2) the test data should be fully understandable and reproducible.

Numerical method is described in the Reference [1].

Test 1. *Fully Expanded Heated Free Jets* ($p_a = p_e$, $T_a = T_e$)

This test aimed at validating the presented turbulence model for the simulation of jets whose temperature, density and pressure at the nozzle exit are the same as those in the ambient, i. e.

$$T_a = T_e, \rho_a = \rho_e, p_a = p_e.$$

This condition makes an estimate of a pure effect of compressibility on jet parameters.

Besides, there is a lot of experimental data available for such kind of jets.

Fig. 1 presents centerline velocity distribution for different values of Mach number M_a. The simulation results (*3*, *4*) were compared with the experimental data of Ref. 14. The increase of nozzle exit Mach number M_a decreases mixing rate of jet with ambient and increases the jet length.

It is difficult experimentally to determine the length of the isentropic zone with sufficient accuracy.

For estimation of jet length it is more convenient to use non-dimensional coordinate $\overline{X}_{0.75} = X_{0.75}/R_a$ — normalized distance from nozzle exit corresponding to the relative velocity $u_C/u_a = 0.75$ (Ref. 15). It should be noted that in accordance with the data of Ref. 14 at Math numbers $M_a = 0.29$, 0.9, and 1.37 the maximum of the turbulent fluctuations and of the gradient of the velocity u_C is observed in the section $\overline{X}_{0.75}$.

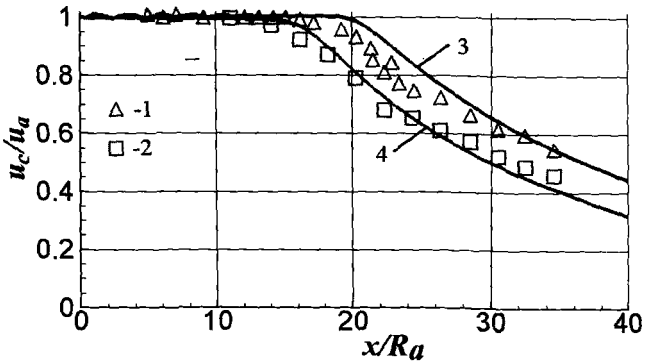

Fig. 1. Test 1. Normalized centerline velocity u_C/u_a vs. normalized distance from nozzle exit x/R_a. *1* — $M_a = 0.9$; *2* — $M_a = 1.37$ — Lau et al. [14] experiment; *3* — $M_a = 0.9$; *4* — $M_a = 1.37$ — predicted distribution

Fig. 2 shows dependence of the relative coordinate $\overline{X}_{0.75}$ on nozzle exit Mach number M_a. The simulation results (curves) were compared with the experimental data of Refs. 14, 15 and 16 (figures). The simulations were performed with the use of the presented turbulence model (curve *5*) and K-ε turbulence model with Sarkar et al. [2] compressibility correction (curve *4*).

Both models are in a good agreement with the experimental data and each other, and also show the increase of the jet length in accordance with the increase of nozzle exit Mach number.

As mentioned above, the presented turbulence model enabled the author to evaluate the effect of

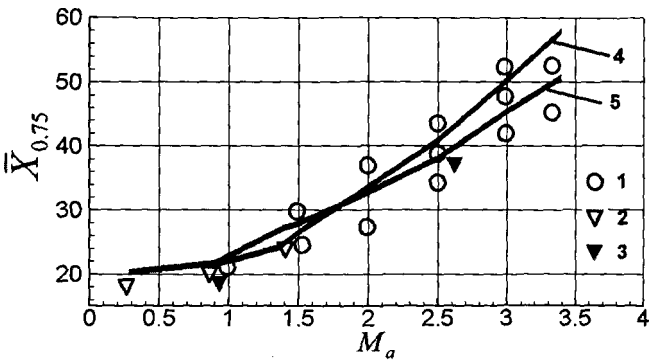

Fig. 2. Test 1. Relative coordinate $\overline{X}_{0.75}$ vs. nozzle exit Mach number M_a. *1*, *2*, *3* — experiment: *1* — data from Krasotkin et al. [15], *2* — data from Lau et al. [14], *3* — data from Glassman and John [16]; *4*, *5* — simulations: *4* — using K-ε turbulence including Sarkar et al. [2] compressibility correction, *5* — present model

Mach number on the distribution of turbulent kinetic energy among its components: $\widetilde{u''^2}, \widetilde{v''^2}, \widetilde{w''^2}$. When jet velocity is small ($M_a = 0.28$) the relation between the normal and tangential components of velocity fluctuations is $\widetilde{v''^2}/\widetilde{u''^2} \approx 0.54$, and when $M_a = 1.37$ — $\widetilde{v''^2}/\widetilde{u''^2} \approx 0.49$. These relations are in satisfactory agreement with Lau et al. [14] data, where they amount at: $\widetilde{v''^2}/\widetilde{u''^2} = 0.45$ —0.55 for $M_a = 0.28$ and $\widetilde{v''^2}/\widetilde{u''^2} = 0.40$ —0.44 for $M_a = 1.37$ at the maximum turbulence regions.

Test 2. Supersonic oxygen jet in high-temperature ambient

This test aimed at investigating the effect of high ambient temperature field on the supersonic oxygen jet behavior. This kind of a flow has great gradients of density and temperature.

For this purpose, simulation was performed for a jet with the following parameters:

$u_a = 451$ m/s; $T_a = 190$ K;
$p_a = 10^5$ Pa, jet fluid — O_2.

Nozzle exit radius: $R_a = 9.2$ mm.

Three variants of ambient parameters were considered:

T_e [K]	$\%O_2$	$\%N_2$	$\%CO_2$
285	54	46	0
772	85	9	6
1002	88	3	9

The simulation results were compared with the experimental data of Sumi et al. [17]. In Ref. 17 supersonic oxygen jet behavior in a high-temperature field was investigated by measuring the velocity, O_2 concentration and temperature of the oxygen jet in a heated furnace.

Fig. 3, *a*—*c* present the distribution of velocity, the concentration of oxygen and temperature on the jet axis at different ambient temperatures. The comparison of the simulation results using the presented method with the experimental data of Sumi et al. [17] shows a good agreement and also demonstrates the fact that the attenuation of the jet is restrained as the ambient temperature increases.

Fig. 4 demonstrates the effect of using variable Pr_T model on the simulation results.

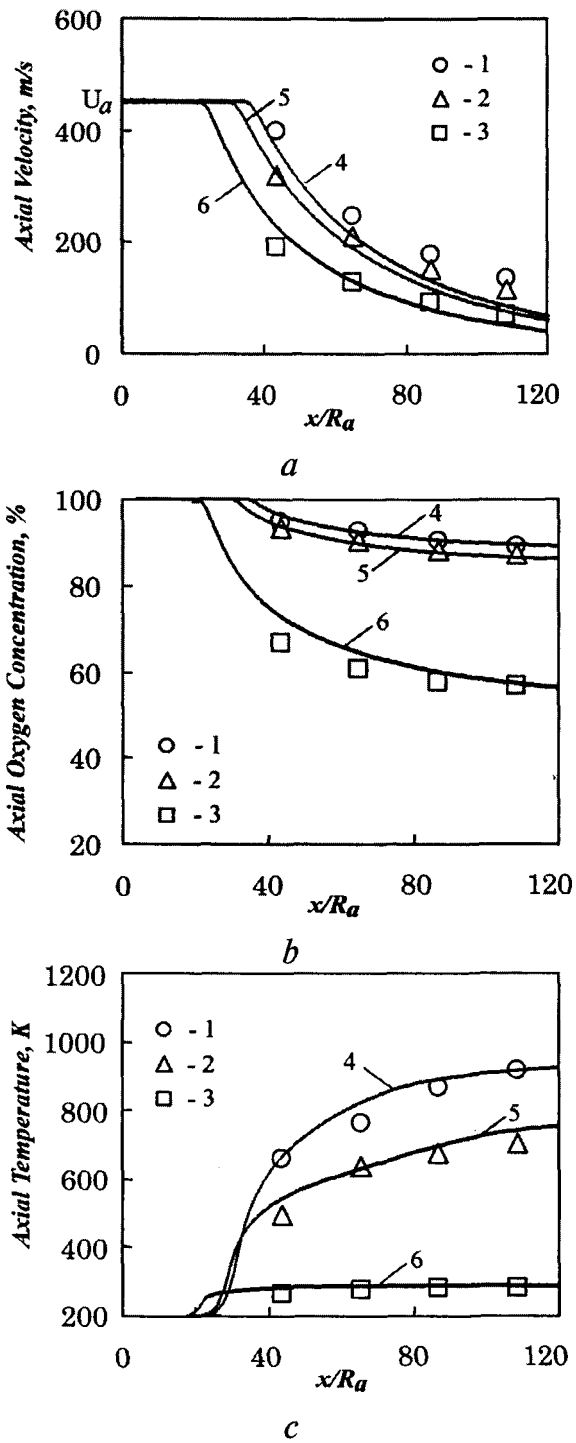

Fig. 3. Test 2. Centerline (*a*) velocity, (*b*) oxygen concentration and (*c*) temperature profiles. *1, 2, 3* — Sumi et al. [17] experiment: *1* — $T_e = 1002$ K, *2* — $T_e = 772$ K, *3* — $T_e = 285$ K; *4, 5, 6* — simulations using present turbulence model: *4* — $T_e = 1002$ K, *5* — $T_e = 772$ K, *6* — $T_e = 285$ K

The variable Pr_T model result is improvement compared with the constant $Pr_T = 0.7$ model.

It may be shown that the noticeable decrease of Pr_T number in the mixing layer causes the oxygen temperature approach faster to the ambient temper-

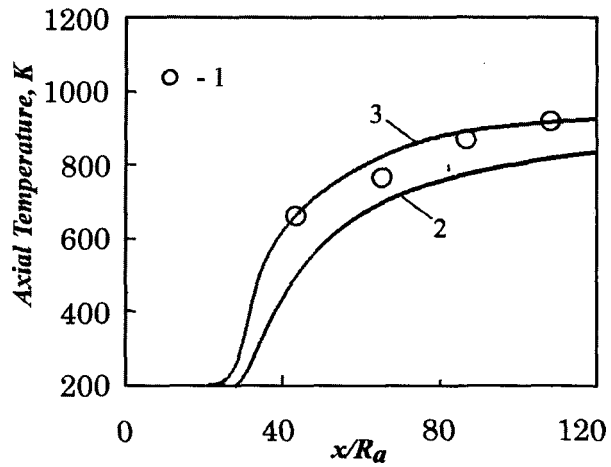

Fig. 4. Test 2. Centerline temperature vs. normalized distance from nozzle exit x/R_a, calculation results for various Pr_T models (constant and variable), T_e = 1002 K. *1* — Sumi et al. [17] experiment; *2*, *3* — simulations: *2* — constant $Pr_T = 0.7$, *3* — variable Pr_T model

ature. This effect only appears at high values of T_e and actually does not influence on velocity distribution.

Test 3. Cold under-expanded and over-expanded air jets at $p_a/p \neq 1$

This test aimed at validating the presented method for under-expanded and over-expanded air jets.

The simulation was performed for air jets having total temperature T_0 = 300 K and nozzle exit Mach number M_a = 3.3. The simulation results were compared with the experimental data of Safronov and Khotulev [18].

Fig. 5, *a*—*c* present the simulation results and the experimental data for an under-expanded jet with static pressure ratio p_a/p_e = 1.5, diameter of the profiled nozzle D_a = 53.7 mm and nozzle exit half cone angle $\theta_a = 10°$.

The simulation was performed using a 400×100 trapezoidal grid. Various turbulence models were used:

1) standard *K*-ε model;

2) *K*-ε turbulence model with compressibility correction of Sarkar et al. [2];

3) *K*-ε turbulence model with compressibility correction of Glebov and Molchanov [4];

4) the turbulence model presented in this paper.

Using standard *K*-ε turbulence model considerably under-predicts the jet length if compared with the experimental data, and also reduces a number of shock diamonds; all shock waves are having significantly lower amplitude than measured.

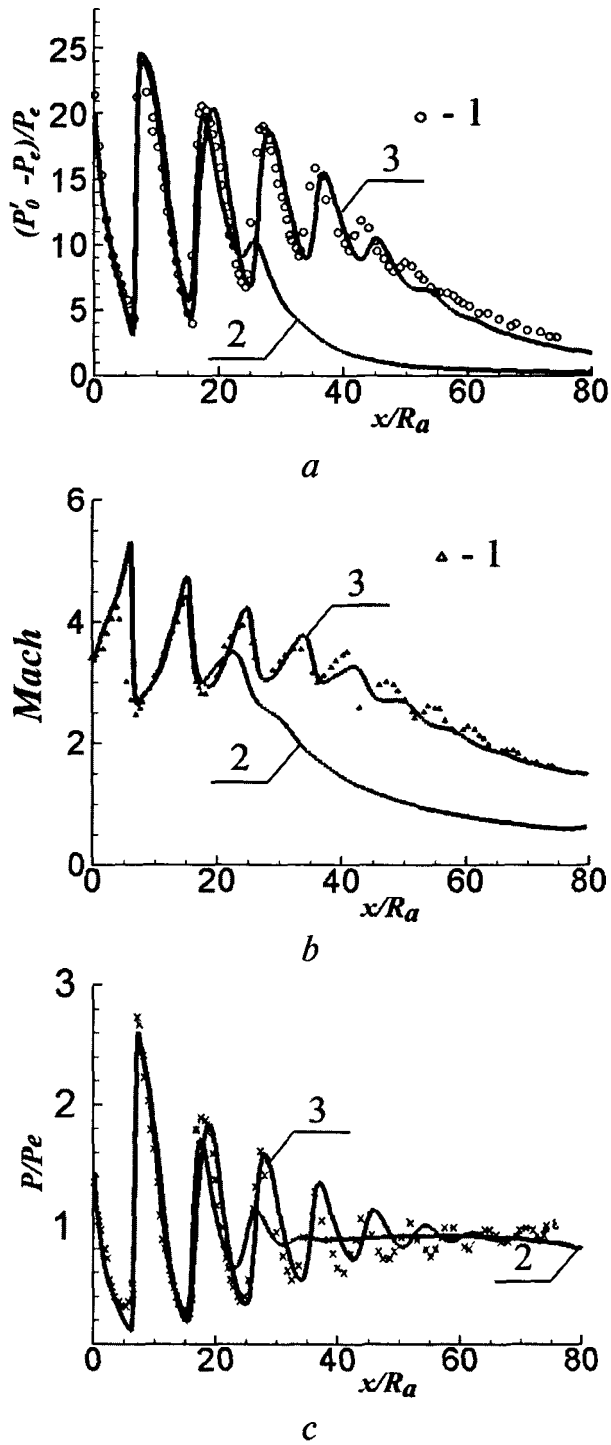

Fig. 5. Test 3. Centerline distribution of *a* — normalized relative pitot pressure, *b* — Mach number and *c* — static pressure in jet with T_0 = 300 K, M_a = 3.3, p_a/p_e 1.5, $\theta_a = 10°$. Calculations using various turbulence models, compared to experiment. *1* — Safronov, Khotulev experiment [18]; *2* — simulation with standard *K*-ε model; *3* — simulation using present mode

Using the other turbulence models (2, 3, 4) gave similar results, which are in a good agreement with the experimental data of Safronov, Khotulev [18].

The pictures only illustrate the simulation results using models 1 and 4.

The similar results were obtained for an over-expanded jet.

Test 4. Supersonic hydrogen jet in supersonic vitiated air coflow

The presented method was applied to the high speed jet flame of Evans et al. [19]. In this experiment, a Mach 2 hydrogen jet was exhausted into a coaxial stream of vitiated air at Mach 1.9. The jet issued from a nozzle with inner diameter $d_j = 0.009525$ m and outer diameter $D = 0.0653$ m. A schematic of the experimental apparatus is shown in Fig. 6.

The test conditions for this case are:

	Hydrogen jet	Free stream
Mach number, M	2.00	1.90
Temperature, T, K	251	1495
Velocity, u, m/s	2432	1510
Pressure, p, MPa	0.1	0.1
Y_{H_2}	1.0	0.0
Y_{O_2}	0.0	0.241
Y_{N_2}	0.0	0.478
Y_{H_2O}	0.0	0.281

Fig. 7, 8 present the axial distributions and radial profiles of species mass fractions obtained though simulation using constant and variable Pr_T, Sc_T models and compared with the Evans et al. [19] data.

The simulated distributions of H_2 and N_2 mass fractions are in a good agreement with the experimental data. The predicted distributions of Prandtl and Schmidt turbulent numbers demonstrate the fact that the values of these parameters increase in the vicinity of flame front, which slightly slows the process of species mixing, shown in fig. 7, 8.

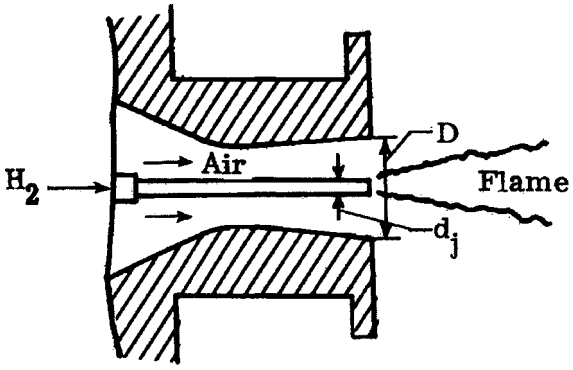

Fig. 6. Test 4. Schematic of the Evans et al. [19] experimental set-up. $D = 0.0653$ m, $d_j = 0.009525$ m, injector lip thickness — 0.0015 m

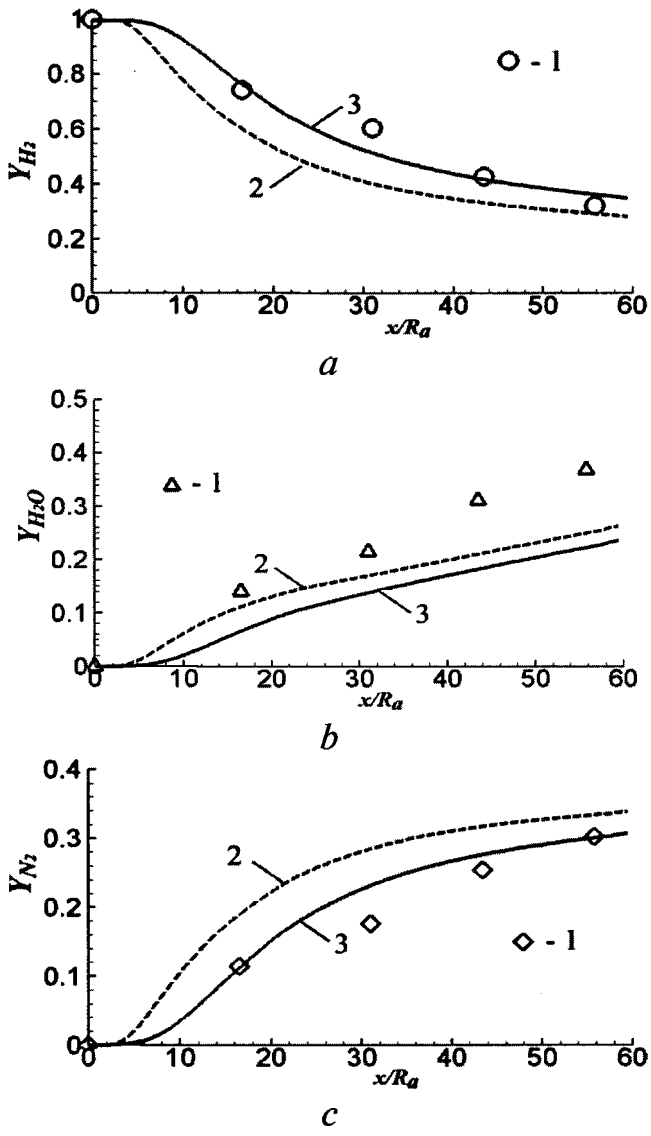

Fig. 7. Test 4. Centerline profiles of *a* — H_2, *b* — H_2O and *c* — N_2 mass fractions. Calculation results (lines) for various Pr_T, Sc_T models (constant and variable) are compared to the experimental data (points). *1* — Evans et al. [19] experiment; *2* — simulation using constant $Pr_T = Sc_T = 0.7$; *3* — simulation using variable Pr_T, Sc_T model

The situation with water mass fraction is worse. This may be accounted for the fact that low-temperature reaction chains including such species as H_2O_2, HO_2 were not considered in the kinetic process of hydrogen burning in the present work. It is assumed that these species are essential for hydrogen ignition.

Test 5. Afterburning of exhaust plume

This test aimed at validating the presented method for investigating of supersonic non-isobaric jets which contain unburned combustible species: H_2,

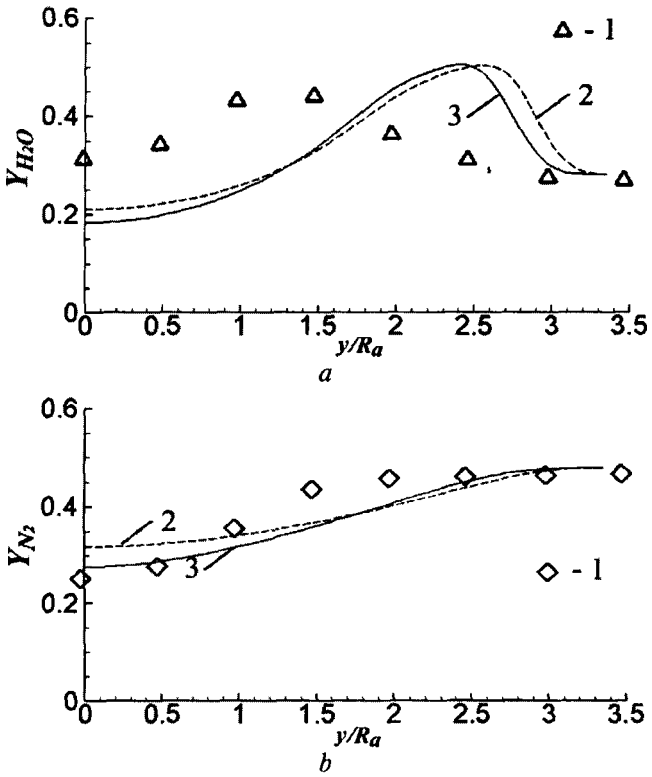

Fig. 8. Test 4. Radial profiles of *a* — H_2O and *b* — N_2 mass fractions. Calculation results (lines) for various Pr_T, Sc_T models (constant and variable) are compared to the experimental data (points). *1* — Evans et al. [19] experiment; *2* — simulation using constant $Pr_T = Sc_T = 0.7$; *3* — simulation using variable Pr_T, Sc_T model

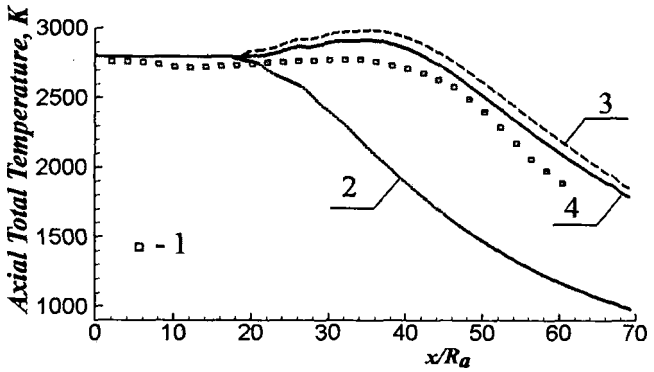

Fig. 10. Test 5. Centerline profile of total temperature in over-expanded jet with $T_0 = 2840$ K, $M_a = 3.24$, $p_a/p_e = 0.73$. Calculation results (lines) for various models are compared to the experimental data (points). *1* — Safronov, Khotulev [18] experiment; *2* — simulation without chemical reactions; *3* — simulation with chemical reactions; *4* — simulation with chemical reactions using variable Pr_T, Sc_T model

CO. These species chemically react with the oxygen contained in air; their afterburning causes a considerable increase of temperature.

This test included the simulation of jets exhausting from hot-gas generator, described in Safronov and Khotulev [18, 20]. Pitot pressure and total temperature were measured.

The numerical investigation for two gas generator operational modes was performed using the same fuel.

Fig. 9 presents centerline distribution of normalized relative pitot pressure in over-expanded jet with the following parameters:

$$T_0 = 2860 \text{ K}, \; M_a = 4.0,$$
$$p_a/p_e = 0.65.$$

Mass fractions of afterburning species are:

$$Y_{H_2} = 0.01; \; Y_{CO} = 0.29.$$

The simulation was carried out with the use of different turbulence models. The simulation results with the presented turbulence model are in a good agreement with the experimental data [20]; using standard *K*-ε model considerably under predicts the jet length; *K*-ε turbulent model with compressibility correction of Sarkar et al. [2] slightly over predicts the jet length.

Fig. 10 shows the comparison of simulation with the experimental

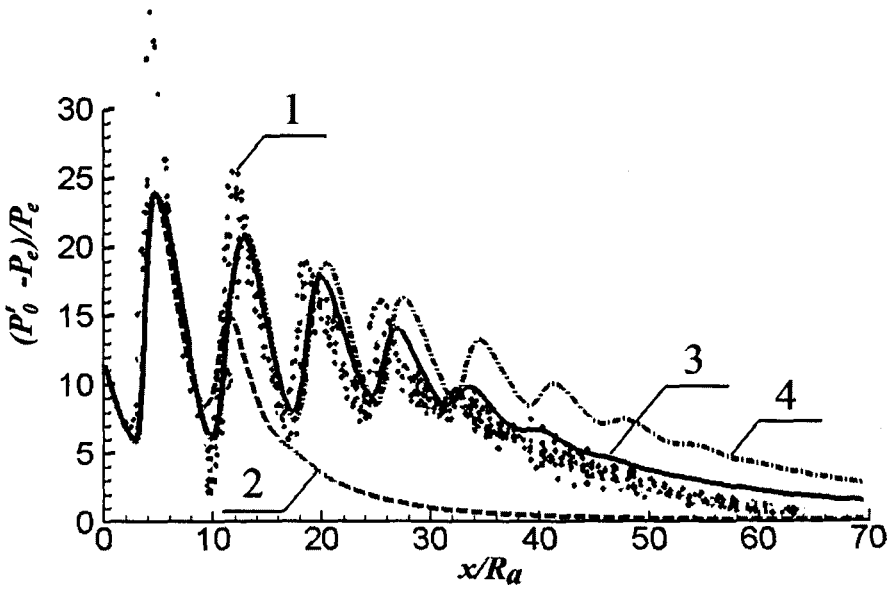

Fig. 9. Test 5. Centerline distribution of normalized relative pitot pressure in overexpanded jet with $T_0 = 2860$ K, $M_a = 4.0$, $p_a/p_e = 0.65$. Calculations using various turbulence models, compared to experiment. *1* — Safronov experiment [20]; *2* — simulation using standard *K*-ε model without compressibility correction; *3* — simulation using present model; *4* — simulation using K-ε model with Sarkar et al. [2] compressibility correction

results of Ref. 18. The same fuel is used, but the conditions at nozzle outlet are slightly different:

$$T_0 = 2840 \text{ K}, \text{M}_a = 3.24, p_a/p_e = 0.73.$$

Mass fraction of afterburning species are:

$$Y_{\text{H}_2} = 0.01; \; Y_{\text{CO}} = 0.29.$$

The investigations which were performed considering the chemical interaction of afterburning species H_2, CO with oxygen are in a general agreement with the experimental data [18]. The variable Pr_T, Sc_T model has improved the predictions. The temperature decreases faster probably owing to the fact that the turbulent Prandtl number is smaller in the afterburning region.

Conclusion

A numerical scheme to solve the fully coupled equations that describe supersonic turbulent jets with non-equilibrium chemical reactions was developed. Scalar variance model to predict variable turbulent Prandtl and Schmidt numbers based on thermodynamic enthalpy and mixture fraction variance concepts has been formulated.

Numerical validation of these jets against experimental measurements of five test cases was performed. Numerical solutions obtained are in satisfactory agreement with experimental data.

The main conclusions are:

1) It is essential to consider compressibility effects on turbulence for the description of jet spreading rate and wave structure.

2) The variable turbulent Prandtl and Schmidt number formulation works well for both reacting and non-reacting flows.

NOMENCLATURE

a — speed of sound;
E — total energy;
H — total enthalpy;
f — scalar value;
$\widetilde{f''^2}$ — scalar value variance;
h — enthalpy;
h_I — species enthalpy;
$J_{I,i}$ — species diffusion flux;
K — turbulent kinetic energy;
M — Mach number;
M_T — turbulent Mach number;
N_C — number of species;
N_R — number of elementary reactions;
N_X, N_Y — number of grid points along ξ-axis and η-axis;
Pr_T — turbulent Prandtl number;
Q_i — heat flux;
p — pressure;
R — universal gas constant;
R_k — rate of elementary reaction k;
Sc_T — turbulent Schmidt number;
T — temperature;
u, v — velocity components in (x, y) coordinates;
V_n'' — velocity fluctuation normal to the streamlines;
W_I — species molecular mass;
Y_I — species mass fraction;
x, y — cartesian coordinates for plain flow, Cylindrical coordinates for axisymmetric flow.

GREEK SYMBOLS

ε — dissipation rate of turbulent kinetic energy;
ε_f — dissipation rate of $\widetilde{f''^2}$
μ_T — turbulent viscosity coefficient;
ρ — density;
ξ, η — generalized coordinate directions;
ω — =0 for plain flow; =1 for axisymmetric flow.

SUBSCRIPTS

0 — Total values of parameters;
a — Nozzle exit;
C — Centerline value;
e — External flow, ambient.

REFERENCES

1. **Molchanov A.M.** Numerical simulation of supersonic chemically reacting turbulent jets // 20th AIAA Computational Fluid Dynamics Conference 27—30 June 2011, Honolulu, Hawaii, AIAA Paper 2011—3211. 37 p.
2. **Sarkar S., Erlebacher G., Hussaini M.Y. and Kreiss H.O.** The analysis and modeling of dilatational terms in compressible turbulence // Journal of Fluid Mechanics. 1991. V. 227. P. 473—493.
3. **Zeman O.** Dilatation dissipation: the concept and application in modeling compressible mixing layer // Physics of Fluids A. 1990. V. 2. P. 178—188.
4. **Glebov G.A. and Molchanov A.M.** Model of turbulence for supersonic reacting jets // Investigation of Heat Transfer in Flying Vehicles (Issledovanie teploobmena v letatelnykh apparatakh). Moscow: Moscow Aviation Institute, 1982. P. 6—11.
5. **El Baz A.M.** Modelling compressibility effects on free turbulent shear flows // 5th Biennial Colloquium on Computational Fluid Dynamics. UMIST, UK. 1992.
6. **Molchanov A.M.** A calculation of supersonic non-isobaric jets with compressibility corrections in a turbulence model // Vestnik MAI. 2009. V. 16. N. 1. P. 38—48.
7. **Kollmann W.** (ed.). Prediction methods for turbulent flows. Hemisphere Pub. Corp., Washington, 1980. 468 p.
8. **Mattick S., Brinckman K.W., Dash S.M. and Liu Z.** Improvements in analyzing high-speed fuel // Air Mixing Problems Using Scalar Fluctuation Modeling, AIAA Paper 2008—768, Jan. 2008.
9. **Baulch D.L., Cobos C.J., Cox R.A., Frank P., Hayman G., Just Th., Kerr J.A., Murrells T., Pilling M.J., Troe J., Walker R.W. and Warnatz J.** Summary table of evaluated

kinetic data for combustion modeling // Combustion and Flame. 1994. V. 98. P. 59—79.
10. **Tsang W., Hampson R.F.** Chemical kinetic data base for combustion chemistry. Part I. Methane and related compounds // Journal of Physical and Chemical Reference Data. 1986. V. 15. 1087 p.
11. **Ibraguimova L.B., Smekhov G.D., Shatalov O.P.** Recommended rate constants of chemical reactions in H_2O_2 gas mixture with electronically excited species O_2 (1), O (1D), OH (2) involved // Physico-chemical kinetics in gas dynamics [online journal]. V. 1. URL: http://www.chemphys.edu.ru/media/files/-2003-01-20-001.pdf [cited 2003].
12. **Lissianski V., Yang H., Qin Z., Mueller M.R., Shin K.S., Gardiner W.C. Jr.** High-temperature measurements of the rate of the coefficient of the H + CO_2 →' CO + OH reaction // Chemical Physics Letters. 1995. V. 240. P. 57—62.
13. **Gardiner W.C. Jr.** (ed.). Combustion chemistry. Springer-Verlag, New York, 1984. 509 p.
14. **Lau J.C., Morris P.J., Fisher M.J.** Measurements in subsonic and supersonic free jets using a laser velocimeter // Journal of Fluid Mechanics. 1979. V. 63. Part 1. P. 1—27.
15. **Krasotkin V.S., Myshanov A.I., Shalaev S.P., Shirokov N.N. and Yudelovich M.Ya.** Investigation of supersonic isobaric submerged turbulent jets // Fluid Dynamics. 1988. V. 23. N 4. P. 529—534.
16. **Glassman I. and John E.A. J.** An unusual aerodynamic stagnation-temperature effect // Journal Aerospace Science. 1959. V. 26. 387 p.
17. **Sumi I., Kishimoto Y., Kikichi Y. and Igarashi H.** Effect of high temperature field on supersonic oxygen jet behavior // ISIJ International. 2006. V. 46. P. 1312—1317.
18. **Safronov A.V., Khotulev V.A.** Results of experimental researches of the supersonic cold and hot jet // Physico-chemical kinetics in gas dynamics [online journal]. V. 6. URL: http://www.chemphys.edu.ru/media/files/2008-10-20-001.pdf, [cited 2008].
19. **Evans J.S., Schexnayder C.J., and Beach H.J.** Application of a two-dimensional parabolic computer program to prediction of turbulent reacting flows // NASA Technical Report NASA TP 1169, 1978.
20. **Safronov A.V.** Jet simulation method of combustion products // Physico-chemical kinetics in gas dynamics [online journal]. V. 4. URL: http://www.chemphys.edu.ru/media/files/2006-10-23-001.pdf, [cited 2006].

ПАМЯТКА АВТОРУ

Автор(ы) статьи передает(ют) ***эксклюзивное право*** издательству ООО "Наука и технологии" на ее публикацию в любой форме в данном журнале и его зарубежных аналогах.

1. К публикации в журнале "Тепловые процессы" принимаются статьи, отвечающие профилю журнала. Статья должна быть подписана **всеми авторами** и датирована. Все страницы должны быть пронумерованы. К статье необходимо приложить акт экспертизы.
2. Изложение материала должно быть ясным, логически выстроенным в следующей последовательности:
а) индекс УДК;
б) название статьи; инициалы и фамилии авторов; место работы, ученое звание и ученая степень каждого из авторов (полное название организации, город, страна, e-mail, телефон);
в) краткая аннотация (не более 3—5 строк, 2—3 предложения);
г) ключевые слова;
д) вводная часть с обоснованием необходимости и изложением цели работы (не более 1 страницы);
е) основной текст (методика эксперимента + экспериментальные результаты и их обсуждение);
ж) выводы, в которых по мере возможности должно быть указано практическое применение результатов;
з) список литературы.
Материалы пунктов б, в, г необходимо представить и на английском языке.
3. Рукопись статьи предоставляется в двух экземплярах, напечатанных на одной стороне стандартного листа формата А4.
4. Набирать текст необходимо в **MS Word**, используя стандартные шрифты ***Times New Roman*** (размер 14) и ***Symbol***, через **полтора** интервала. Поля со всех сторон 20 мм.
5. Для набора формул следует использовать встроенный редактор формул ***Math Equation*** или встраиваемый формульный процессор ***Math Type***. Формулы в тексте должны быть напечатаны без дополнительных интервалов между строками текста. Нумеруются только те формулы, на которые есть ссылки в тексте.
6. **Все** используемые в тексте буквенные обозначения и аббревиатуры должны быть расшифрованы. Размерность величин должна соответствовать системе СИ.
7. Один из экземпляров рукописи размечается. Буквы латинского алфавита в формулах и в тексте размечаются простым карандашом: прописные буквы нужно подчеркнуть двумя чертами снизу; строчные — двумя чертами сверху. Показатели степени, надстрочные знаки и верхние индексы следует описать дугой снизу; нижние — дугой сверху. Математические символы типа lim, cos, max, общепринятые обозначения вида Re, Fe и др., число 0, а также русские буквы в индексах необходимо подчеркнуть квадратной скобкой снизу (⌴). Греческие буквы обводятся красным карандашом. Аргументы функций необходимо брать в скобки или отделять от обозначения функций пробелом.
8. Элементы списка литературы должны содержать фамилии и инициалы авторов, полное название работы. Для книг указывается место издания, издательство, год издания и количество страниц. Для статей — название журнала или сборника, год выпуска, том, номер, номера первой и последней страниц.
9. Подписи к рисункам выполняются на отдельной странице, также включенной в общую нумерацию текста статьи.
10. Графический материал только в **черно-белом** изображении должен быть четким и не требовать перерисовки.
11. Каждый рисунок распечатывается на отдельной странице, на которой внизу указываются его порядковый номер, автор и название статьи.
12. Таблицы должны иметь названия, их следует прилагать после статьи, каждую на отдельной странице.
13. К статье следует приложить диск с файлами: текста статьи, таблиц, подписей к рисункам и самих рисунков (изображение выполняется в форматах ***jpeg*** или ***tiff*** с разрешением не менее ***300 dpi***), аннотации с названием статьи и фамилиями авторов на русском и английском языках.
14. В сведениях об авторах следует сообщить: ФИО (полностью); дату рождения (число, месяц, год); домашний адрес фактического проживания с указанием почтового индекса; домашний и служебный телефоны (с кодом города); e-mail.

Плата за публикацию статей с авторов, в том числе с аспирантов, не взимается.
Статью направлять в адрес редакции: 107076, г. Москва, Стромынский пер., 4, оф. 410.
Изд-во "Наука и технологии". Журнал "Тепловые процессы".